
ACTIVE INFERENCE MEETING ENERGY-EFFICIENT CONTROL OF PARALLEL AND IDENTICAL MACHINES

A PREPRINT

Yavar Taheri Yeganeh
Politecnico di Milano
yavar.taheri@polimi.it

Mohsen Jafari
Rutgers University
jafari@soe.rutgers.edu

Andrea Matta
Politecnico di Milano
andrea.matta@polimi.it

June 14, 2024

Abstract

We investigate the application of active inference in developing energy-efficient control agents for manufacturing systems. Active inference, rooted in neuroscience, provides a unified probabilistic framework integrating perception, learning, and action, with inherent uncertainty quantification elements. Our study explores deep active inference, an emerging field that combines deep learning with the active inference decision-making framework. Leveraging a deep active inference agent, we focus on controlling parallel and identical machine workstations to enhance energy efficiency. We address challenges posed by the problem's stochastic nature and delayed policy response by introducing tailored enhancements to existing agent architectures. Specifically, we introduce multi-step transition and hybrid horizon methods to mitigate the need for complex planning. Our experimental results demonstrate the effectiveness of these enhancements and highlight the potential of the active inference-based approach.

Keywords Active Inference · Probabilistic Deep Learning · Reinforcement Learning · Energy-Efficient Control · Manufacturing Systems

1 Introduction

Active inference (AIF), an emerging field inspired by the principles of biological brains, offers a promising alternative for decision-making models. It unifies perception, learning, and decision-making under the free energy principle (FEP), which formulates neuronal inference and learning under uncertainty [1]. Accordingly, the brain is modeled through levels of (variational) Bayesian inference [2], minimizing prediction errors by leveraging a generative model of the world while considering uncertainties. This framework enables the development of agents that can calibrate their models and make decisions without complete knowledge of system dynamics. Significant progress has been made in applying active inference across various domains, including robotics, autonomous driving, and healthcare [3, 4, 5], showcasing its ability to handle complex decision-making tasks in dynamic environments.

Recently, the manufacturing industry's focus on energy efficiency has intensified due to its significant contribution to global energy consumption. Addressing energy efficiency at the machine level has become critical, with energy-efficient scheduling (EES) and energy-efficient control (EEC) strategies emerging as key approaches to reducing environmental impact [6]. While traditional EEC methods often necessitate complete system knowledge, reinforcement learning (RL) has shown potential in optimizing manufacturing processes without prior system knowledge [7, 8]. However, RL agents may struggle to rapidly adjust their policies to changing conditions.

This research aims to build upon advancements in active inference-based decision-making [9, 10] and apply it to EEC in manufacturing systems, demonstrating its potential and advancing the understanding of active inference in complex environments. The existing active inference agents often rely on extensive search

algorithms during planning and make decisions based on immediate next predictions [9], which pose challenges in the context of the EEC problem. By employing deep active inference as the decision-making algorithm, we introduce tailored enhancements, such as multi-step transition and hybrid horizon methods, to address the challenges posed by the problem’s stochastic nature and delayed policy response. Our experimental results highlight the effectiveness of these enhancements and underscore the potential of the active inference-based approach. The remainder of the paper is organized as follows: we begin by concisely introducing the EEC problem and the manufacturing system under study. We then present an overview of the formalization of active inference, describe the agent, evaluate its performance, and discuss future directions.

2 Application Overview

Active inference has proven effective in various applications commonly associated with decision-making processes in biological agents, such as humans and animals. These applications primarily involve visual sensory output as observations. For instance, Fountas et al. (2020) [9] tested their agent on tasks like *Dynamic dSprites* [11] and *Animal-AI* [12], which can be performed by biological agents simply. Additionally, applications in robotics [13, 14] (e.g., manipulation [4]) align with tasks that human agents can typically perform naturally. This effectiveness stems from active inference being a theory of decision-making for biological agents [2]. However, certain applications, such as the control of industrial systems, can present complex challenges. While the decision-making processes and existing applications mentioned above may not be straightforward, human agents may struggle to devise effective policies for these more intricate problems.

2.1 EEC in Manufacturing Systems

EEC gaining prominence in both academic and industrial circles within manufacturing systems. It offers substantial energy savings across three key control levels: component, machine, and production system. At its core, EEC involves managing the power consumption state of objects based on environmental conditions. Objects are kept fully operational when their functions are needed and transitioned to low power states when not in use, though this poses challenges due to the unpredictable nature of environmental demands and the penalties incurred during state transitions. These penalties include both time wasted during transition, when the object adds no value, and the energy consumed during the transition process. A comprehensive and recent literature review on this topic can be found in [15].

2.2 System Description

The specific system under study is a manufacturing workstation consisting of a single upstream buffer serving multiple parallel machines as depicted in Fig. 1. Key characteristics of this system include a finite buffer capacity, stochastic arrival of parts, and identical machines operating in a mass-production context. Each machine can exist in various states including working, standby, startup, and failed, with further subdivisions within the working state to denote idle and busy states. Additionally, machines are subject to stochastic failures and repairs, each with expected durations, further complicating control strategies. Power consumption

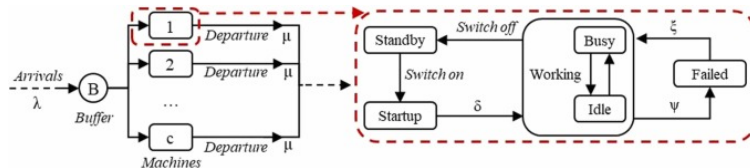


Figure 1: Layout of parallel machines.

varies based on the machine’s state, with different power requirements for standby, startup, idle, and busy states. For instance, standby and failed states require minimal power consumption, while idle and startup states demand higher levels. Furthermore, the highest power consumption occurs during the busy state when the machine is fully operational and actively processing parts. Managing these power variations efficiently is crucial for effective energy-efficient control in manufacturing systems.

3 Deep Active Inference Agent

Active inference is a unifying theory that integrates inference, perception, and action by emphasizing the dependence of observations on actions [16]. To effectively manage observations toward preferred states, the optimization of actions plays a crucial role [16]. This concept was originally proposed as a framework for understanding how organisms actively control and navigate their environment by iteratively updating their beliefs and actions based on sensory evidence [2]. The FEP [17, 18] is at the core of active inference, paving the way for creating a mathematical model, and there are even experimental evidences supporting it [19]. We modify the proposed agent by Fountas et al. (2020) [9], which exhibited notable capabilities and performance when compared against three benchmark model-free RL algorithms in two image applications.

3.1 Active Inference Formalism

Active inference agents employ an integrated probabilistic framework consisting of an internal generative model [10] coupled with inference mechanisms to represent and interact with the world. Similar to RL the agent interacts with the environment, but using three random variables representing observation, latent state, and action (i.e., (o_t, s_t, a_t) at time t). The framework assumes a Partially Observable Markov Decision Process (POMDP) [20, 10, 21]. The generative model of the agent, parameterized with θ , is defined over these variables (i.e., $P_\theta(o_{1:t}, s_{1:t}, a_{1:t-1})$) [9]. Generally, the agent acts to reduce *surprise*, which can be quantified by $-\log P_\theta(o_t)$. Specifically, there are two steps for the agent while interacting with the world [2, 9] as follows:

1) The agent calibrates its generative model through fitting predictions and improve its representation of the world. This is done by minimizing Variational Free Energy (VFE), which is similar to *surprise* of predictions in connection with the actual observations [9, 22, 21], as follows:

$$\theta^* = \arg \min_{\theta} \left(\mathbb{E}_{Q_\phi(s_t, a_t)} [\log Q_\phi(s_t, a_t) - \log P_\theta(o_t, s_t, a_t)] \right) . \quad (1)$$

This objective function is commonly known as the negative evidence lower bound (ELBO) [23], which is the upper bound for $-\log P_\theta(o_t)$. It is also used as a foundation for training variational autoencoders [24].

2) The agent makes decisions (i.e., chooses actions) in active inference based on the accumulated negative Expected Free Energy (EFE or G):

$$P(\pi) = \sigma(-G(\pi)) = \sigma \left(- \sum_{\tau > t} G(\pi, \tau) \right) , \quad (2)$$

where $\sigma(\cdot)$ represents the *Softmax* function, and π (i.e., policy) denotes the sequence of actions. The EFE encompasses minimizing *surprise* regarding preferred observations¹, exploring uncertainty, and reducing uncertainty about model parameters [9]. The EFE for $\tau \geq t$ can be formulated as follows [25]:

$$G(\pi, \tau) = \mathbb{E}_{P(\sigma_\tau | s_\tau, \theta)} \mathbb{E}_{Q_\phi(s_\tau, \theta | \pi)} [\log Q_\phi(s_\tau, \theta | \pi) - \log P(o_\tau, s_\tau, \theta | \pi)] . \quad (3)$$

Fountas et al., (2020) [9] provided a derivation [25] for calculating the EFE in Eq. 3 at each time step:

$$G(\pi, \tau) = -\mathbb{E}_{\tilde{Q}} [\log P(o_\tau | \pi)] \quad (4a)$$

$$+ \mathbb{E}_{\tilde{Q}} [\log Q(s_\tau | \pi) - \log P(s_\tau | o_\tau, \pi)] \quad (4b)$$

$$+ \mathbb{E}_{\tilde{Q}} [\log Q(\theta | s_\tau, \pi) - \log P(\theta | s_\tau, o_\tau, \pi)] . \quad (4c)$$

They expanded the formalism, leading to a tractable estimate for EFE that is both interpretable and calculable [9]:

$$G(\pi, \tau) = -\mathbb{E}_{Q(\theta | \pi) Q(s_\tau | \theta, \pi) Q(o_\tau | s_\tau, \theta, \pi)} [\log P(o_\tau | \pi)] \quad (5a)$$

$$+ \mathbb{E}_{Q(\theta | \pi)} \left[\mathbb{E}_{Q(o_\tau | \theta, \pi)} H(s_\tau | o_\tau, \pi) - H(s_\tau | \pi) \right] \quad (5b)$$

$$+ \mathbb{E}_{Q(\theta | \pi) Q(s_\tau | \theta, \pi)} H(o_\tau | s_\tau, \theta, \pi) - \mathbb{E}_{Q(s_\tau | \pi)} H(o_\tau | s_\tau, \pi) . \quad (5c)$$

This paved the way for establishing a unified formalism for computing decisions in Eq. 2. Accordingly, actions are connected to perception, which is achieved through Bayesian inference, based on the EFE in Eq. 5.

¹Here, the *surprise* refers to the preference, while in VFE, *surprise* pertains to the actual observation used for calibrating the model.



Figure 2: The illustration depicts two views of the active inference framework: general steps on the left and active inference elements on the right.

Through this formalism that leads to calculating the EFE (i.e., Eq. 5), we can interpret the contribution of each element [9]: **The first term** (i.e., Eq. 5a) is analogous to reward in RL as it is the *surprise*² of the prediction considering preferred observation. **The second term** (i.e., Eq. 5b) represents state uncertainty, which is mutual information between the agent’s beliefs about state before and after prediction. This term also shows a motivation to explore areas of the environment that resolve state uncertainty [9]. **The third term** (i.e., Eq. 5c) represents uncertainty about model parameters considering new observations. This term is also referred active learning, novelty, or curiosity [9]. In fact, model parameters (i.e., θ), particularly contribute to making predictions, including generation of the next states.

In summary, the framework (as depicted in Fig. 2) is realized through a mathematical formalism in the following manner. The observation is fed as input, which propagates through the model to create perception (i.e., beliefs), which include generating future states. It is to facilitate the calculation of EFE (in Eq. 5) integrated into the planner derived from policy (in Eq. 2) to act on the environment. After obtaining the next observation the VFE (in Eq. 1) can be calculated, which calibrate (i.e., learning) the model based on the matching the new observation with the prediction. In fact, every time the framework goes through the loop the model is optimized based on the VFE form the previous loop, then the optimized model is used to for the rest.

3.2 Architecture

An agent within the active inference framework needs different modules, which are entangled within the framework. Amortization [26, 27] is introduced into the formalism (in Sec. 3.1) to scale-up the realization [9]. The formalism is inherently probabilistic and parameterized with with two sets, $\theta = \{\theta_s, \theta_o\}$ representing generative and $\phi = \{\phi_s\}$ recognition elements [9]. Using the following parameterized modules the formalism (in Sec. 3.1) can be calculated: **Encoder** (i.e., $Q_{\phi_s}(s_t)$), an amortized inference of the hidden state (i.e., an inference network [28] providing a mapping between the observation, \tilde{o}_t , and a distribution for its corresponding hidden state). **Transition** (i.e., $P_{\theta_s}(s_{t+1}|\tilde{s}_t, \tilde{a}_t)$), which generates a distribution for the next hidden state based on both a sampled action and the current hidden state. **Decoder** (i.e., $P_{\theta_o}(o_{t+1}|\tilde{s}_{t+1})$) generates a distribution for prediction based on the sampled hidden state.

Neural networks can facilitate the realization of these modules by representing a mapping between a sample and the respective distribution. In fact, parameters of a pre-selected (e.g., Gaussian) distribution can be approximated. Here, we model the state space specifically with a multivariate Gaussian distribution, assuming no covariance (i.e., diagonal Gaussian). Using the VFE (i.e., Eq. 1), all the three networks can be trained in an end to end fashion. Aside from action and the transition, which can even be considered integrated within the state space, the structure bears a resemblance to a variational autoencoder [24]. It is noteworthy that training for the both include optimizing ELBO, as specified in Eq. 1.

Utilizing the mentioned architecture (also depicted in Fig. 3), the agent would be able to calculate the EFE in Eq. 5 for a given policy (i.e., π), which is a sequence of actions. Thus, we can calculate the probabilities for selecting actions through Eq. 2. In order to make better decisions, the agent can plan ahead by simulating future trajectories using the architecture mentioned above. However, as the policy space grows exponentially into the future, it is infeasible to evaluate all possible scenarios. Fountas et al. (2020) [9] introduced two approaches to alleviate the obstacle. 1) They used the standard Monte-Carlo Tree Search (MCTS) [29, 30], a

²Here, instead of maximizing cumulative rewards, the focus is on minimizing the *surprise*, which quantifies the extent of deviation (i.e., misalignment) between the prediction and the preferred observation.

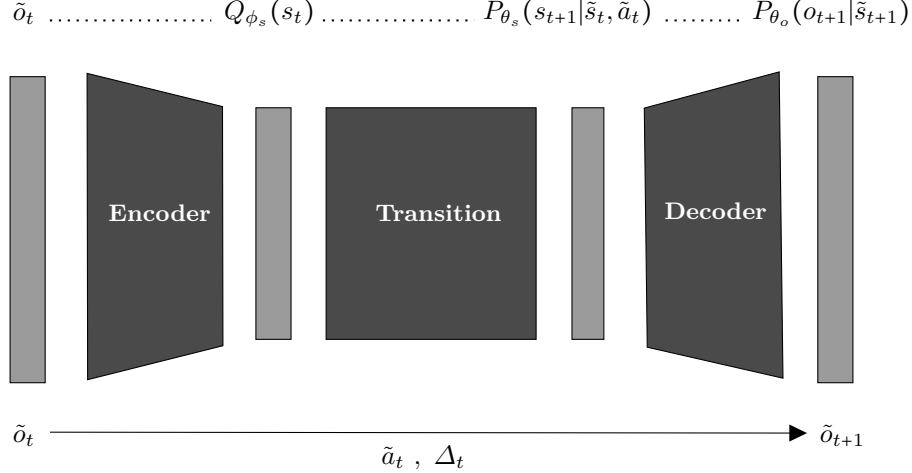


Figure 3: The agent’s architecture and generative framework resemble that of a VAE. The line on top represents the agent simulating the future and making a prediction, while on the bottom, the agent receives a new observation after Δ_t of taking an action, \tilde{a}_t .

tree-based search algorithm, which selectively explore promising trajectories in a restricted manner. 2) They introduced another recognition module [31, 32, 27], parameterized with ϕ_a as follows: **Habit** (i.e., $Q_{\phi_a}(a_t)$), an amortized inference of actions (i.e., an inference network [28] providing a mapping between a sampled hidden state, \tilde{s}_t , and normalized, through *Softmax* function, probabilities for the actions). Habit is also realized through a neural network, which approximates the posterior distribution over actions (i.e., $P(a_t|s_t)$) using the prior $P(a_t)$ that is obtained from the MCTS [9]. This network is trained to reproduce the last action sampled from the planner, given the last state. This is similar to the fast and habitual decision-making in biological agents [33].

Fountas et al. (2020) [9] followed the standard four steps of MCTS [34], which let them to restrict and prioritize the trajectories that should be evaluated. Iteratively a weighted tree that has memory updates the visited states. During each loop, a path from the existing tree (towards a leaf node) is selected (i.e., **selection**) based on the following upper bound confidence:

$$U(s_t, a_t) = \tilde{G}(s_t, a_t) + c_{\text{explore}} \cdot Q_{\phi_a}(a_t|s_t) \cdot \frac{1}{1 + N(a_t, s_t)} \quad (6)$$

Where $\tilde{G}(s_t, a_t)$ represents the algorithm’s current estimation for the EFE, while $N(a_t, s_t)$ denotes the number of times a node (i.e., a state and action pair) in the tree has been visited during the tenure, along with an exploration hyperparameter, c_{explore} . Then, starting from the leaf and for every possible action (i.e., **expansion**), the EFE is calculated for a fixed number of future steps (i.e., **simulation**). This value is finally added to all nodes along the path to calculate the average of $\tilde{G}(s_t, a_t)$ (i.e., **backpropagation**). After all, Actions are sampled from the probabilities created by $P(a_t) = \frac{N(a_t, s_t)}{\sum_j N(a_t, j, s_t)}$ (where $P(a_t) = \sum_{\pi: a_1=a_t} P(\pi)$), which is proportional to the number of times a node is visited. The planning process continues until a maximum number of loops (i.e., a hyperparameter) is reached, or a condition, i.e., $\max P(a_t) - \text{mean} P(a_t) > T_{\text{dec}}$, is met, indicating that the planning is finished. Fountas et al. (2020) [9] further employed $Q_{\phi_a}(a_t)$ (i.e., habit) to modulate the state space, motivated by incorporating uncertainty. The divergence between the policy obtained from the planner (i.e., MCTS) and the habit (i.e., $D_t = D_{\text{KL}}[Q_{\phi_a}(a_t) || P(a_t)]$) can serve as a loss function for the habit. This divergence also represents a type of uncertainty in the state space, preventing the habit from being identical to the policy [35, 36]. Therefore, they used D_t in a logistic function as follows:

$$\omega_t = \frac{\alpha}{1 + e^{-\frac{b-D_{t-1}}{c}}} + d. \quad (7)$$

The monotonically decreasing pattern establishes a reciprocal connection between D_{t-1} and ω_t , i.e., the state precision, using hyperparameters $\{\alpha, b, c, d\}$. Altogether, the transition (i.e., $P_{\theta_s}(s_t|s_{t-1}, a_{t-1})$) is modeled with the distribution $\mathcal{N}(\mu, \sigma^2/\omega_t)$ [9]. This precision is analogous to β in β -VAE [11], effectively promoting disentanglement of the state space by the encoder [9].

To facilitate the computations and effectively estimating different elements within the framework, Fountas et al. (2020) [9] used several levels of Monte-Carlo simulations (i.e., sampling based estimations). In addition to

MCTS, all terms in the EFE (Eq. 5), including the use of MC dropout [37] for model parameters (i.e., 5c), are estimated in this manner [9].

3.3 Enhancements

We explore various aspects to design the agent and leverage the formalism and existing architecture outlined by Fountas et al. (2020) [9] as a foundation. First, we examine how features and requirements related to the problem under study can influence the agent. Subsequently, we propose solutions to address these issues, introducing a coherent agent design.

3.3.1 Exploring the Application

The simulation of the system, described in Section 2.1, is designed to replicate features of an industrial system. It utilizes Poisson processes [38] (i.e., exponential distributions) for machine state transitions and part arrivals [7]. The *event-driven* steps employed by Loffredo et al. (2023) [7, 8] trigger decisions after a system state transition rather than at fixed intervals, proving effective for controlling working machines. This problem can be viewed as either continuous-time stochastic control or a discrete-time Markov Chain process [39]. Continuous-time modeling requires making time intervals visible to the agent for both machines and subsequent observations, whereas discrete-time modeling allows the agent to learn dynamics by observing transitions to create probabilities for different transitions. There is a variable time interval between subsequent observations (i.e., Δt as depicted in Fig. 3). This variability requires synchronizing the transition for prediction (i.e., $P_{\theta_o}(o_{t+1}|\tilde{s}_{t+1})$) with the next observation (i.e., \tilde{o}_{t+1}) in the continuous-time model. Incorporating continuous-time facilitates neural network function approximation for longer Δt during planning. However, using continuous-time can further complicate the prediction structure since residence times for machine states exist in observation. Here, we utilize discrete-time *event-driven* steps that simplify this process compared to the continuous-time approach.

The stochastic nature and the integral and continuous form of the reward functions for the system under study [7, 8] mean decision impacts may not be immediately observable, aligning with POMDPs. The system has a delay in responding to the policy, which we call a *long/delayed impact horizon*, particularly with respect to reward. This is an important distinction from environments evaluated by Fountas et al. (2020) [9]. The agent proposed by them focuses on planning based on immediate next predictions. The problem at hand is continuous with no terminal state, and the span over which reward functions are integrated may encompass a few thousand steps. This complicates planning and highlights the need for less computational cost.

3.3.2 Experience Replay

The generative model encompasses the core of active inference [17, 2, 9] and predictive coding [16]. Therefore, the performance of any active inference-based agent heavily relies on its accuracy. To improve model training, we introduce experience replay [40] using a memory that stores (o_t, a_t, o_{t+1}) at different steps. During training, we sample a batch of experiences from the memory and ensure the latest experience is also included. However, for all the batched experiences, we utilize ω_t based on the latest experience.

3.3.3 Hybrid Horizon

To address the limitations arising from the short horizon of the EFE, which relies on immediate next predictions, we propose augmenting the planner with an auxiliary term to account for longer horizons. Q-learning [41] and its enhanced variant, deep Q-learning, can serve as model-free planners with longer horizons, leveraging rewards to update the Q-value for a state-action pair [42]. Loffredo et al. (2023) [9] demonstrated that deep Q-learning can achieve near-optimal performance for the systems under study. Accordingly, we modify $Q_{\phi_a}(a_t)$ to represent amortized inference of actions, mapping observations \tilde{o}_t (or sampled predictions) to normalized action probabilities using a *Softmax* function and training it with deep Q-learning updates based on rewards coming from experience replay. We introduce a hyperparameter γ to balance the contributions of long and short horizons. Thus, we arrive at a new formulation for the planner to incorporate longer horizons:

$$P(a_t) = \gamma \cdot Q_{\phi_a}(a_t) + (1 - \gamma) \cdot \sigma(-G(\pi)). \quad (8)$$

The resulting combination achieves a controlled balance between the EFE for the short horizon terms, which incorporates uncertainties, and the long horizon term. We further utilize the new $Q_{\phi_a}(a_t)$ to modulate the agent’s state uncertainty based on Eq. 7. In fact, D_t (i.e., $D_{\text{KL}}[Q_{\phi_a}(a_t) \| P(a_t)]$) represents the discrepancy between the long horizon and the combined policy, reflecting a form of knowledge gap for the agent.

3.3.4 Multi-Step Transition and Planning

Given the stochastic nature and *long impact horizon* of the system under study, a one-step transition (as depicted in Fig. 3) may not result in significant changes in observation and state, leading to indistinguishable EFE terms. Therefore, the model should learn transitions beyond one step and predict further into the future to distinguish the impact of different policies. We modify the transition module to allow multiple steps, controlled by a hyperparameter (e.g., $s = 90$), enabling multi-step transitions given the policy (i.e., sequence of actions). Representing the sequence of actions in a policy as a one-hot vector can be high-dimensional, so we utilize integer encodings as an approximation. This is feasible since the actions (or number of machines) are less categorical and can be considered rather continuous in this case. During planning, we utilize repeated actions in the transition for each action and calculate the EFE accordingly. This method assesses the impact of actions over a short period, using repeated action simulations. This approximation helps to distinguish different actions over a horizon based on the EFE. Thus, even a single multi-step transition can serve as a simple and computationally efficient planner. For deeper simulations, it can be combined with MCTS of repeated transitions. Alternatively, it can be combined with a less expensive planner that starts with repeated transitions for each action, followed by simulating until a specific depth using the following policy:

$$\tilde{P}(\pi, a_\tau) = (1 - c_{\text{explore}}) \cdot Q_{\phi_a}(a_\tau) + c_{\text{explore}} \cdot \sigma(-\log P(o_\tau|\pi)), \quad (9)$$

to calculate the EFE of the final state or trajectory. After several loops, the accumulated EFE for each action can be used in Eq. 8.

4 Results

To demonstrate the potential of our methodology, we concentrate our experiments on controlling a real industrial workstation comprising six parallel-identical machines with an upstream capacity of 10, as outlined in [7]. All the stochastic processes characterizing the workstation follow Poisson distributions, and thus are exponentially distributed with different expected values. We first introduce the preference function, then describe the setup and training, and finally present the numerical performance of our agent³.

4.1 Preference Function

Active inference involves an agent acting to achieve its preferred observation, similar to the concept of a setpoint in control theory [35, 16]. Consequently, the agent possesses an internal function to quantify the proximity of the prediction to the preferred state. This function is important for the agent’s performance. While it correlates with the reward function in reinforcement learning, it is based on a different philosophy: a control setpoint rather than the cumulative reward in the MDP framework of reinforcement learning [42]. Instead of the reward function used by Loffredo et al. (2023) [8], we propose a different preference function for the multi-objective optimization of the system under study. This function aligns with the concept of a *long/delayed impact horizon* system for our agent to control, accounting for the average performance of the system over a fixed time span (t_s^4 , e.g., 8 hours) leading up to the observation at (t). It includes terms for production, energy consumption, and a combined term as follows:

$$R_{\text{production}} = \frac{T_{\text{current}}}{T_{\text{max}}} \quad (10a)$$

$$R_{\text{energy}} = 1 - \frac{E_{\text{avg}}}{E_{\text{max}}} \quad (10b)$$

$$R = \phi \cdot R_{\text{production}} + (1 - \phi) \cdot R_{\text{energy}}, \quad (10c)$$

where:

- ϕ is the weighting coefficient balancing production and energy consumption. It is set close to 1 (0.97 in our implementation) to ensure that the agent does not significantly reduce production.
- $T_{\text{current}} = \frac{NP(t) - NP(t - t_s)}{t_s}$ represents the throughput within the past t_s period, where $NP(t)$ is the number of parts produced within this period.
- T_{max} is the maximum achievable throughput, occurring under the *ALL ON* policy [8].

³The source code will be available on GitHub at https://github.com/YavarYeganeh/AIF_Meeting_EEC.

⁴In our implementation, we use the closest recorded timestamp from the system, respecting the fixed time span.

- $E_{\text{avg}} = \frac{C(t) - C(t - t_s)}{t_s}$ represents the average energy consumption over the past t_s period, where $C(t)$ is the total energy consumption within this period.
- E_{max} is the maximum theoretical consumption rate of the system, pertaining to all machines operating in their busy state.

4.2 Agent Setup and Training

We adhere to the MC sampling methodology for calculating EFE, as well as most agent configurations, as outlined by Fountas et al. (2020) [9]. Notably, we employ Bernoulli and Gaussian distributions to model prediction and state distributions, respectively. We introduced a modification by utilizing activation functions for the encoder and transition networks. The output of these two networks generates means and variances representing Gaussian distributions for the state. We applied the *Tangent Hyperbolic* function for the means and the *Sigmoid* function, multiplied by a factor, λ_s , between 1 and 2, for the variances. This enforces further regularization and stability for the state space to prevent unbounded values, which need to be fitted into a normal distribution. In our implementation, in contrast to [9], which does not use activations for the state, these activations are essential for learning an effective policy.

Our agent’s observation comprises buffer levels and machine states, all one-hot encoded. Similarly, we incorporate the three reward terms in Eq. 10, predicting only their means without pre-defining a distribution. The agent’s preference (i.e., $P(o_\tau | \pi)$) corresponds to the prediction of the combined reward term for the system, which the agent seeks to maximize. Given the composition of binary and continuous components of the observation, the loss of the VAE’s reconstruction is equally scaled aggregation of binary cross-entropy and mean square error. Additionally, due to the one-hot structure of the observation, we sample the predictions, excluding the reward terms, which are treated as means, to be fed into the decoder during the calculation of EFE. As we validate the performance of a control system for an industrial application, we use a single system during each training epoch, with an experience replay size of 200. These systems are initialized with a random policy for one day of simulation, after removing the profile from one day of warm-up simulation using the *ALL ON* policy. We trained our agents on-policy, following a similar approach to the algorithm proposed by Fountas et al. (2020) [9], but with adjustments to accommodate the modifications we made, including multi-step transition, experience replay, and a hybrid planner.

4.3 Agent Performance

To assess the efficacy of our agents, we tested their performance several times during different training epochs, each on independent systems initialized with a random agent after warm-up, similar to those used for training. We simulated the interaction between the agent and the system, which was randomly controlled at the beginning, for one day of simulation time. The combined reward term (in Eq. 10) at the end of the test simulation was extracted as the performance measure, with a time span of t_s (i.e., 8 hours in this case). Our agent, similar to [9], has a large set of hyperparameters, which proved to be sensitive, especially those related to the state space of the model. We considered both 1-step transitions and multi-step transitions, taking repeated actions during planning for each of the possible actions (i.e., determining how many machines to keep *ON*) to then calculate their EFE. Fig. 4 presents the comparison for a single set of hyperparameters, particularly $\lambda_s = 1$, except s , across different γ . It shows the suitability of the multi-step transition and simple repeated planner as well as hybrid horizon.

Since the state should fit the normal distribution, $\lambda_s = 1$ for variance will target areas of the input domain of the *Sigmoid* function that are saturated and have smaller gradients. To address this, we increased λ_s to 1.5, where the *Sigmoid* function has larger gradients. This results in higher rewards even for very small γ (i.e., 0.05), as presented in Fig. 5. This performance is primarily coming from the second term of the EFE (i.e., Eq. 5b), which serves as an *intrinsic reward* [21], as demonstrated in Fig. 5C. The other two terms are less distinguishable for different actions on average. This suggests that the agent differentiates between various actions in its state space to achieve high rewards. In fact, the *long impact horizon* and stochasticity, as well as our approximations in transition and planning, hinder the predictive power of the agent, but it managed to infer the impact of different actions in its state space. It is also worth noting that our agent quickly converges to high rewards but may experience instability and loss of control if training continues for (a long time), due to a *catastrophic* increase in the loss, particularly the reconstruction term of the generative model. This necessitates early stopping mechanisms for training and the introduction of regularization elements (e.g., dropout and normalization) to prevent or mitigate the issue.

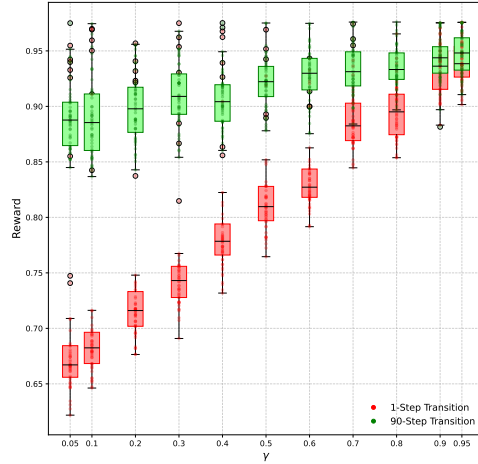


Figure 4: Comparison of test rewards during training of agents with 90-step transition against 1-step transition, when $\lambda_s = 1$.

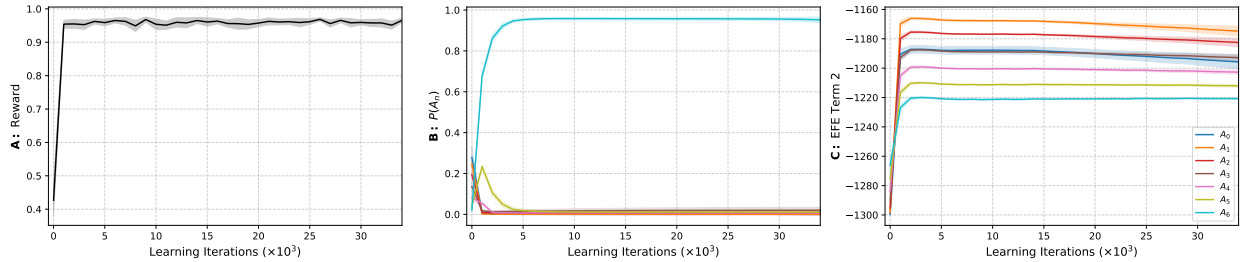


Figure 5: The test performance of the agent with 90-step transition and repeated actions for planning, when $\lambda_s = 1.5$ and $\gamma = 0.05$, replicated with 10 different random seeds. **A**: Average reward. **B**: Average planner distribution for different actions. **C**: Average EFE’s term 2 for different actions.

5 Conclusion and Future Work

The results of our study demonstrate the effectiveness of our proposed modifications for the active-inference-inspired agent. Notably, a single multi-transition lookahead with repeated actions, coupled with a hybrid horizon, can achieve high rewards without the need for extensive planning algorithms like MCTS. This is particularly notable considering the unique challenges posed by the application under study, which demands deep lookahead into the future to distinguish different actions, while stochasticity presents a challenge. The significant impact of hyperparameters on agent performance emphasizes the importance of meticulous tuning for optimal results and effective control. This highlights the potential of our methodology to tackle the EEC problem and similar applications characterized by a *long/delayed impact horizon* and high stochasticity.

Improving the methodology can involve enhancing the generative model, the core of active inference, especially by introducing recurrent transitions or enhancing predictive capabilities. Integration of diffusion-based generative models instead of VAEs [5] is also a promising direction. The framework and formalism of active inference agents show promise for non-stationary scenarios, where model-free agents may struggle to adapt swiftly. Future research will concentrate on improving the agent, extending experimental validation, and tailoring the methodology to non-stationary scenarios, leveraging the strengths of active inference to develop more robust and efficient decision-making algorithms.

References

- [1] Karl Friston. The free-energy principle: a unified brain theory? *Nature reviews neuroscience*, 11(2): 127–138, 2010. 1
- [2] Thomas Parr, Giovanni Pezzulo, and Karl J Friston. *Active inference: the free energy principle in mind, brain, and behavior*. MIT Press, 2022. 1, 2, 3, 6
- [3] Corrado Pezzato, Carlos Hernández Corbato, Stefan Bonhof, and Martijn Wisse. Active inference and behavior trees for reactive action planning and execution in robotics. *IEEE Transactions on Robotics*, 39(2):1050–1069, 2023. 1
- [4] Tim Schneider, Boris Belousov, Georgia Chalvatzaki, Diego Romeres, Devesh K Jha, and Jan Peters. Active exploration for robotic manipulation. In *2022 IEEE/RSJ International Conference on Intelligent Robots and Systems (IROS)*, pages 9355–9362. IEEE, 2022. 1, 2
- [5] Yufei Huang, Yulin Li, Andrea Matta, and Mohsen Jafari. Navigating autonomous vehicle on unmarked roads with diffusion-based motion prediction and active inference. *arXiv preprint arXiv:2406.00211*, 2024. 1, 9
- [6] Alberto Loffredo, Nicola Frigerio, Ettore Lanzarone, and Andrea Matta. Energy-efficient control in multi-stage production lines with parallel machine workstations and production constraints. *IIEE Transactions*, 56(1):69–83, 2024. 1
- [7] Alberto Loffredo, Marvin Carl May, Louis Schäfer, Andrea Matta, and Gisela Lanza. Reinforcement learning for energy-efficient control of parallel and identical machines. *CIRP Journal of Manufacturing Science and Technology*, 44:91–103, 2023. ISSN 1755-5817. 1, 6, 7
- [8] Alberto Loffredo, Marvin Carl May, Andrea Matta, and Gisela Lanza. Reinforcement learning for sustainability enhancement of production lines. *Journal of Intelligent Manufacturing*, pages 1–17, 2023. 1, 6, 7
- [9] Z. Fountas, Noor Sajid, Pedro A. M. Mediano, and Karl J. Friston. Deep active inference agents using monte-carlo methods. *ArXiv*, abs/2006.04176, 2020. 1, 2, 3, 4, 5, 6, 8
- [10] Lancelot Da Costa, Noor Sajid, Thomas Parr, Karl Friston, and Ryan Smith. Reward maximization through discrete active inference. *Neural Computation*, 35(5):807–852, 2023. 1, 3
- [11] Irina Higgins, Loic Matthey, Arka Pal, Christopher Burgess, Xavier Glorot, Matthew Botvinick, Shakir Mohamed, and Alexander Lerchner. beta-vae: Learning basic visual concepts with a constrained variational framework. In *International conference on learning representations*, 2016. 2, 5
- [12] Matthew Crosby, Benjamin Beyret, and Marta Halina. The animal-ai olympics. *Nature Machine Intelligence*, 1(5):257–257, 2019. 2
- [13] Pablo Lanillos, Cristian Meo, Corrado Pezzato, Ajith Anil Meera, Mohamed Baioumy, Wataru Ohata, Alexander Tschantz, Beren Millidge, Martijn Wisse, Christopher L Buckley, et al. Active inference in robotics and artificial agents: Survey and challenges. *arXiv preprint arXiv:2112.01871*, 2021. 2
- [14] Lancelot Da Costa, Pablo Lanillos, Noor Sajid, Karl Friston, and Shujhat Khan. How active inference could help revolutionise robotics. *Entropy*, 24(3):361, 2022. 2
- [15] Paolo Renna and Sergio Materi. A literature review of energy efficiency and sustainability in manufacturing systems. *Applied Sciences*, 11(16):7366, 2021. 2
- [16] Beren Millidge, Tommaso Salvatori, Yuhang Song, Rafal Bogacz, and Thomas Lukasiewicz. Predictive coding: towards a future of deep learning beyond backpropagation? *arXiv preprint arXiv:2202.09467*, 2022. 3, 6, 7
- [17] Karl Friston, Francesco Rigoli, Dimitri Ognibene, Christoph Mathys, Thomas Fitzgerald, and Giovanni Pezzulo. Action and behavior: A free-energy formulation. *Biological Cybernetics*, 102(3):227–260, 2010. 3, 6
- [18] Beren Millidge. Applications of the free energy principle to machine learning and neuroscience. *arXiv preprint arXiv:2107.00140*, 2021. 3
- [19] Takuya Isomura, Kiyoshi Kotani, Yasuhiko Jimbo, and Karl J Friston. Experimental validation of the free-energy principle with in vitro neural networks. *Nature Communications*, 14(1):4547, 2023. 3
- [20] Leslie Pack Kaelbling, Michael L Littman, and Anthony R Cassandra. Planning and acting in partially observable stochastic domains. *Artificial intelligence*, 101(1-2):99–134, 1998. 3

-
- [21] Aswin Paul, Noor Sajid, Lancelot Da Costa, and Adeel Razi. On efficient computation in active inference. *arXiv preprint arXiv:2307.00504*, 2023. 3, 8
- [22] Noor Sajid, Francesco Faccio, Lancelot Da Costa, Thomas Parr, Jürgen Schmidhuber, and Karl Friston. Bayesian brains and the rényi divergence. *Neural Computation*, 34(4):829–855, 2022. 3
- [23] David M Blei, Alp Kucukelbir, and Jon D McAuliffe. Variational inference: A review for statisticians. *Journal of the American statistical Association*, 112(518):859–877, 2017. 3
- [24] Diederik P Kingma and Max Welling. Auto-encoding variational bayes. *arXiv preprint arXiv:1312.6114*, 2013. 3, 4
- [25] Philipp Schwartenbeck, Johannes Passecker, Tobias U Hauser, Thomas HB FitzGerald, Martin Kronbichler, and Karl J Friston. Computational mechanisms of curiosity and goal-directed exploration. *elife*, 8:e41703, 2019. 3
- [26] Samuel Gershman and Noah Goodman. Amortized inference in probabilistic reasoning. In *Proceedings of the annual meeting of the cognitive science society*, volume 36, 2014. 4
- [27] Joe Marino, Yisong Yue, and Stephan Mandt. Iterative amortized inference. In *International Conference on Machine Learning*, pages 3403–3412. PMLR, 2018. 4, 5
- [28] Charles C Margossian and David M Blei. Amortized variational inference: When and why? *arXiv preprint arXiv:2307.11018*, 2023. 4, 5
- [29] David Silver, Julian Schrittwieser, Karen Simonyan, Ioannis Antonoglou, Aja Huang, Arthur Guez, Thomas Hubert, Lucas Baker, Matthew Lai, Adrian Bolton, et al. Mastering the game of go without human knowledge. *nature*, 550(7676):354–359, 2017. 4
- [30] Rémi Coulom. Efficient selectivity and backup operators in monte-carlo tree search. In *International conference on computers and games*, pages 72–83. Springer, 2006. 4
- [31] Alexandre Piché, Valentin Thomas, Cyril Ibrahim, Yoshua Bengio, and Chris Pal. Probabilistic planning with sequential monte carlo methods. In *International Conference on Learning Representations*, 2018. 5
- [32] Alexander Tschantz, Beren Millidge, Anil K Seth, and Christopher L Buckley. Control as hybrid inference. *arXiv preprint arXiv:2007.05838*, 2020. 5
- [33] Matthijs Van Der Meer, Zeb Kurth-Nelson, and A David Redish. Information processing in decision-making systems. *The Neuroscientist*, 18(4):342–359, 2012. 5
- [34] Maciej Świechowski, Konrad Godlewski, Bartosz Sawicki, and Jacek Mańdziuk. Monte carlo tree search: A review of recent modifications and applications. *Artificial Intelligence Review*, 56(3):2497–2562, 2023. 5
- [35] Karl Friston, Thomas FitzGerald, Francesco Rigoli, Philipp Schwartenbeck, and Giovanni Pezzulo. Active inference: a process theory. *Neural computation*, 29(1):1–49, 2017. 5, 7
- [36] Anna Byers and John T Serences. Exploring the relationship between perceptual learning and top-down attentional control. *Vision research*, 74:30–39, 2012. 5
- [37] Yarín Gal and Zoubin Ghahramani. Dropout as a bayesian approximation: Representing model uncertainty in deep learning. In *international conference on machine learning*, pages 1050–1059. PMLR, 2016. 6
- [38] John Frank Charles Kingman. *Poisson processes*, volume 3. Clarendon Press, 1992. 6
- [39] Sheldon M Ross. *Introduction to probability models*. Academic press, 2014. 6
- [40] Volodymyr Mnih, Koray Kavukcuoglu, David Silver, Andrei A Rusu, Joel Veness, Marc G Bellemare, Alex Graves, Martin Riedmiller, Andreas K Fidjeland, Georg Ostrovski, et al. Human-level control through deep reinforcement learning. *nature*, 518(7540):529–533, 2015. 6
- [41] Christopher JCH Watkins and Peter Dayan. Q-learning. *Machine learning*, 8:279–292, 1992. 6
- [42] Richard S Sutton and Andrew G Barto. *Reinforcement learning: An introduction*. MIT press, 2018. 6, 7